Synthesis, Magnetic Properties, and Incomplete Double-Cubane Structure of Manganese(III)−Metal(II) Complexes [Mn(MeOH)L(OH)M(bpy)]$_2$ (M = Zn, Cu, Ni, and Mn; H_4L = 1,2-Bis(2-hydroxybenzamido)benzene; bpy = 2,2′-Bipyridine)

Yukinari Sunatsuki,[†] Hiromitsu Shimada,[†] Toshihiro Matsuo,[†] Masaaki Nakamura,[†] Fumiaki Kai,[†] Naohide Matsumoto,*[,†] and Nazzareno Re[‡]

Department of Chemistry, Faculty of Science, Kumamoto University, Kurokami 2-39-1, Kumamoto 860-8555, Japan, and Dipartmento di Chimica, Universita di Perugia, via Elce di Sotto 8, 06100 Perugia, Italy

Received May 14, 1998

The manganese(III) complex K[MnL(py)$_2$]·py (H_4L = 1,2-bis(2-hydroxybenzamido)benzene, py = pyridine) reacted as a ligand complex at the two phenoxo oxygen atoms with metal(II) ion and 2,2′-bipyridine to give a series of heterometal complexes [Mn(MeOH)L(OH)M(bpy)]$_2$ (M(II) = Zn (**1**); Cu (**2**); Ni (**3**); Mn (**4**)). X-ray structures were determined **1**, $C_{68}H_{74}N_8O_{18}Mn_2Zn_2$: a = 12.367(3) Å, b = 12.844(2) Å, c = 12.262(2) Å, α = 106.58(1)°, β = 117.89(1)°, γ = 78.57(2)°, triclinic, $P\bar{1}$, and Z = 1. **2**, $C_{68}H_{74}N_8O_{18}Mn_2Cu_2$: a = 13.447(1) Å, b = 12.670-(2) Å, c = 21.732(1) Å, β = 107.076(5)°, monoclinic, $P2_1/n$, and Z =2. **3**, $C_{68}H_{74}N_8O_{18}Mn_2Ni_2$: a = 12.358(3) Å, b = 12.847(3) Å, c = 12.315(3) Å, α = 106.63(2)°, β = 118.71(1)°, γ = 78.32(2)°, triclinic, $P\bar{1}$, and Z = 1. **4**, $C_{66}H_{66}N_8O_{16}Mn_4$: a = 12.511(2) Å, b = 21.129(3) Å, c = 12.811(1) Å, β = 110.12(1)°, monoclinic, $P2_1/n$, and Z = 2. The X-ray analyses confirmed that each of the crystals consists of an incomplete double-cubane molecule with a [$Mn_2M_2O_6$] core, in which two M(II) ions are bridged by two hydroxo groups to form a planar dinuclear moiety bridged by di-μ-hydroxo groups [(bpy)M(OH)$_2$M(bpy)]$^{2+}$ and the dinuclear moiety is sandwiched between two Mn(III) complexes [Mn(MeOH)L]$^-$. The Mn(III) ion and the dinuclear M(II) moiety are triply bridged by the one hydroxo oxygen of the dinuclear moiety and two phenoxo oxygen atoms of the Mn(III) ligand complex. The two phenoxo oxygen atoms of the Mn(III) ligand complex coordinate as an axial ligand to two independent metal(II) ions of the dinuclear moiety. The magnetic susceptibilities of **1**−**4** were measured in the temperature range of 2−300 K. All the Mn(III) ions in these complexes are in a high-spin state of S_{Mn} = 2 with a d^4 electronic configuration, and the metal(II) ions are in the spin states of S_{Zn} = 0, S_{Cu} = 1/2, S_{Ni} = 1, and $S_{Mn(II)}$ = 1/2 (low-spin). The magnetic susceptibility data are well reproduced by the following spin Hamiltonian based on the rhombus spin coupling model with spin (S_1, S_2, S_3, S_4) = (2, S_M, 2, S_M), including a zero-field splitting term for the Mn(III) centers: $\mathbf{H} = g_{Mn}\beta(\mathbf{S}_1 + \mathbf{S}_3)\cdot\mathbf{H} + g_M\beta(\mathbf{S}_2 + \mathbf{S}_4)\cdot\mathbf{H} - 2J(\mathbf{S}_1\cdot\mathbf{S}_2 + \mathbf{S}_2\cdot\mathbf{S}_3 + \mathbf{S}_3\cdot\mathbf{S}_4 + \mathbf{S}_4\cdot\mathbf{S}_1) - 2J'(\mathbf{S}_2\cdot\mathbf{S}_4) + D_{Mn}[\mathbf{S}_{1z}^2 + \mathbf{S}_{3z}^2]$, in which g_{Mn} and g_M are the g factors of the Mn(III) and M(II) ions, J and J' are the Mn(III)−M(II) and M(II)−M(II) Heisenberg coupling constants, and D is the zero-field splitting parameter of Mn(III). The calculated best-fit parameters are as follows: g_{Mn} = 1.91, g_{Cu} = 2.39, J = −4.5 cm^{-1}, J' = −8.1 cm^{-1}, and D_{Mn} = −4.9 cm^{-1} for **2**; g_{Mn} = 1.97, g_{Ni} = 2.23, J = −1.5 cm^{-1}, J' = −2.6 cm^{-1}, and D_{Mn} = −5.5 cm^{-1} for **3**; and g_{Mn} =1.95, $g_{Mn(II)}$ = 2.29, J = −3.5 cm^{-1}, J' = −14.1 cm^{-1}, and D_{Mn} = −12.0 cm^{-1} for **4**. The spin frustration due to the incomplete double-cubane structure is discussed.

Introduction

There has been continuous interest in the study of multinuclear metal complexes with the aims to elucidate the magnetic coupling between paramagnetic metal ions,[1] to mimic the active centers of some biological metalloenzymes,[2] and to produce new functional materials such as a molecular magnet.[3]

Among the multinuclear metal complexes, the field of heterometal polynuclear complexes is still limited by the small number of known and fully characterized compounds and by the relative difficulty of synthesizing such new compounds.[4] Two synthetic strategies have been developed for the synthesis of heterometal complexes. One uses a multinucleating ligand providing two or more unequivalent coordination environments

* To whom correspondence should be addressed.
[†] Kumamoto University.
[‡] Universita di Perugia.

(1) (a) Kahn, O. *Molecular Magnetism*; VCH: Weinheim, Germany, 1993. (b) *Magnetic Molecular Materials*; Gatteschi, D., Kahn, O., Miller, J. S., Palacio, F., Eds.; NATO ASI Series E; Kluwer Academic: Dordrecht, The Netherlands, 1991; Vol. 198. (c) Kahn, O. *Struct. Bonding* **1987**, *67*, 89.

(2) (a) Colman, J. P. *Inorg. Chem.* **1997**, *36*, 5145. (b) Mizoguchi, T. J.; Lippard, S. J. *Inorg. Chem.* **1997**, *36*, 4526. (c) Wang, Y.; DuBois, J. L.; Hedman, B.; Hodgson, K. O.; Stack, T. D. P. *Science* **1998**, *279*, 537. (d) Sträter, N.; Lipscomb, W. N.; Klabunde, T.; Krebs, B. *Angew. Chem., Int. Ed. Engl.* **1996**, *35*, 2024. (e) Frey, S. T.; Murthy, N. N.; Weintraub, S. T.; Thompson, L. K.; Karlin, K. D. *Inorg. Chem.* **1997**, *36*, 956. (f) Karlin, K. D.; Cruse, R. W.; Gultneh, Y.; Hayes, J. C.; Zubieta, J. *J. Am. Chem. Soc.* **1984**, *106*, 3372. (g) Halfen, J. A.; Mahapatra, S.; Wilkinson, E. C.; Kaderli, S.; Young, V. G., Jr.; Que, L., Jr.; Zuberbühler, A. D.; Tolman, W. B. *Science* **1996**, *271*, 1397.

(3) (a) Sato, O.; Iyoda, T.; Fujishima, A.; Hashimoto, K. *Science* **1996**, *271*, 49. (b) Entley, W. R.; Girolami, G. S. *Science* **1995**, *268*, 397. (c) Gleizes, A.; Verdaguer, M. *J. Am. Chem. Soc.* **1981**, *103*, 7373. (d) Kahn, O.; Galy, J.; Journaux, Y.; Morgenstern-Badarau, I. *J. Am. Chem. Soc.* **1982**, *104*, 2165. (e) Miyasaka, H.; Matsumoto, N.; Okawa, H.; Re, N.; Gallo, E.; Floriani, C. *J. Am. Chem. Soc.* **1996**, *118*, 981.

10.1021/ic980543y CCC: $15.00
Published on Web 09/26/1998

for different metal ions.[5] The other uses a "ligand complex" exhibiting coordination ability to metal ions.[6] The "ligand complex" method is effective and advantageous for the synthesis of hetero metal complexes with the systematic combination of metal ions, because the complex can function just like a ligand to a variety of metal complexes exhibiting an extra-acceptable and/or substitutable coordination site.

Previously, Sunatsuki et al.[7] studied the dianionic nickel(II) and copper(II) complexes with a tetraanionic tetradentate ligand, where the ligand is 1,2-bis(2-hydroxybenzamido)benzene, hereafter abbreviated as H_4L. It was revealed that (1) these dianionic complexes have two amido oxygens and two phenoxo oxygens atoms per complex and these donor atoms could function as donor coordination atoms to the other metal ion and (2) the complexes reacted with several metal(II) ions and terminal capping ligands such as 2,2′-bipyridine (bpy) to produce a series of dinuclear homo- and heterometal complexes bridged by the di-μ-phenoxo moiety as well as the cyclic, tetranuclear complexes bridged by di-μ-phenoxo-μ-amido moieties (Scheme 1).

If either of the functional donor atoms, the charge of the complex, the metal ion, and the capping ligand in this ligand complex system were modified, it would be expected that new multinuclear complexes with a variety of nuclearities, extended structures, and bridging modes could be obtained. From this viewpoint, the manganese(III) complex with the same ligand was selected for the synthesis of heterometal polynuclear complexes in this study, since the coordination chemistry of manganese(III) is distinctly different from that of copper(II) and nickel(II). As anticipated, the manganese(III) complex functioned as a distinctly different ligand complex from those of the copper(II) and nickel(II) counterparts. The manganese(III) complex reacted with 2,2′-bipyridine as a capping ligand and metal(II) ion to give a series of tetranuclear manganese(III)−metal(II) complexes with the chemical formulas $[Mn(MeOH)L(OH)M(bpy)]_2$ (M = Zn (**1**); Cu (**2**); Ni (**3**); Mn (**4**)) (Scheme 2). Here we report the synthesis, characterization, unique incomplete double-cubane structure, and magnetic properties of these complexes.

Scheme 1

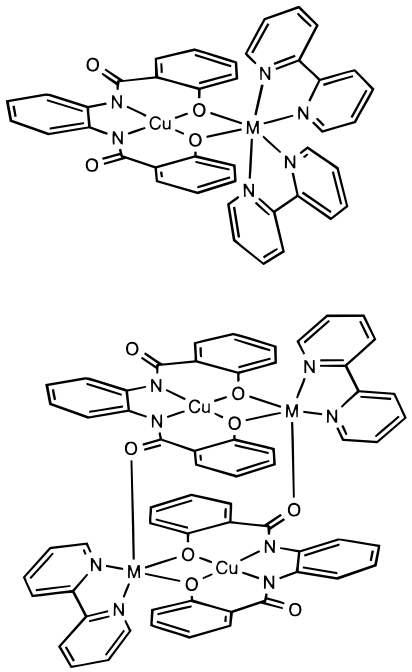

Scheme 2

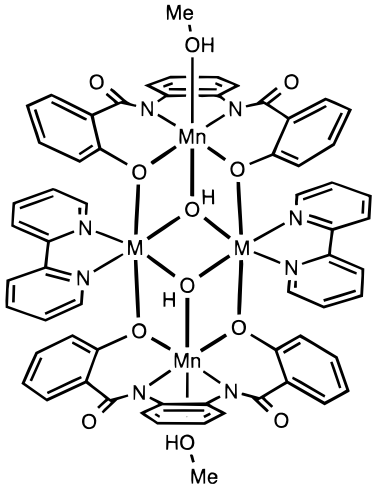

Experimental Section

General Procedures. All chemicals and solvents used for the syntheses were reagent grade. Reagents used for the physical measurements were spectroscopic grade. A tetradentate ligand, 1,2-bis(2-hydroxybenzamido)benzene, abbreviated H_4L, was prepared according

(4) (a) Bentini, A.; Bentini, C.; Caneschi, A.; Carlin, R. L.; Dey, A.; Gatteschi, D. *J. Am. Chem. Soc.* **1985**, *107*, 8128. (b) Sans, J. L.; Ruiz, R.; Gleizes, A.; Lloret, F.; Fans, J.; Julve, M.; Borrás-Almenar, J. J.; Journaux, Y. *Inorg. Chem.* **1996**, *35*, 7384. (c) Costes, J.-P.; Laurent, J.-P.; Sanchez, J. M. M.; Varela, J. S.; Ahlgren, M.; Sundberg, M. *Inorg. Chem.* **1997**, *36*, 4646. (d) Burdinski, D.; Birkelbach, F.; Weyhermüller, T.; Flörke, U.; Haupt, H.-J.; Lengen, M.; Trautwein, A. X.; Bill, E.; Wieghardt, K.; Chaudhuri, P. *Inorg. Chem.* **1998**, *37*, 1009.

(5) (a) Fenton, D. E.; Lintvedt, R. L. *J. Am. Chem. Soc.* **1978**, *100*, 6367. (b) Mazurek, W.; Berry, K. J.; Murry, K. S.; O'Connor, M. J.; Snow, S. J.; Wedd, A. G. *Inorg. Chem.* **1982**, *21*, 3071. (c) Gagné, R. R.; Spiro, C. L.; Smith, T. J.; Hamann, C. A.; Thies, W. R.; Shiemke, A. K. *J. Am. Chem. Soc.* **1981**, *103*, 4073. (d) McCollum, D. G.; Yap, G. P. A.; Rheingold, A. L.; Bosnich, B. *J. Am. Chem. Soc.* **1996**, *118*, 1365. (e) Thompson, L. K.; Tandon, S. S.; Manuel, M. E. *Inorg. Chem.* **1995**, *34*, 2356. (f) Aratake, Y.; Okawa, H.; Asato, E.; Sakiyama, H.; Kodera, M.; Kida, S.; Sakamoto, M. *J. Chem. Soc., Dalton Trans.* **1990**, 2941. (g) Mohanta, S.; Nanda, K. K.; Werner, R.; Haase, W.; Mukherjee, A. K.; Dutta, S. K.; Nag, K. *Inorg. Chem.* **1997**, *36*, 4656.

(6) (a) Costes, J.-P.; Dahan, F.; Laurent, J.-P. *J. Chem. Soc., Dalton Trans.* **1989**, 1017. (b) Costes, J.-P.; Dahan, F.; Dupuis, A.; Laurent, J.-P. *Inorg. Chem.* **1996**, *35*, 2400. (c) O'Bryan, N. B.; Maier, T. O.; Paul, I. C.; Drago, R. S. *J. Am. Chem. Soc.* **1973**, *95*, 6640. (d) Baron, V.; Gillon, B.; Plantevin, O.; Cousson, A.; Mathoniere, C.; Kahn, O.; Grand, A.; Öhrström, L.; Delley, B. *J. Am. Chem. Soc.* **1996**, *118*, 11822. (e) Larionova, J.; Chavan, S. A.; Yakhmi, J. V.; Frøystein, A. G.; Sletten, J.; Sourisseau, C.; Kahn, O. *Inorg. Chem.* **1997**, *36*, 6374. (f) Pei, Y.; Kahn, O. *J. Am. Chem. Soc.* **1986**, *108*, 3143. (g) Sinn, E.; Harris, M. *Coord. Chem. Rev.* **1969**, *4*, 391. (h) Ruiz, R.; Julve, M.; Faus, J.; Lloret, F.; Muñoz, M. C.; Journaux, Y.; Bois, C. *Inorg. Chem.* **1997**, *36*, 3434. (i) Gordon-Wylie, S. W.; Bominaar, E. L.; Collins, T. J.; Workman, J. M.; Claus, B. L.; Patterson, R. E.; Williams, S. A.; Conklin, B. J.; Yee, G. T.; Weintraub, S. T. *Chem. Eur. J.* **1995**, *1*, 528. (j) Nozaki, T.; Ushio, H.; Mago, G.; Matsumoto, N.; Okawa, H.; Yamakawa, Y.; Anno, T.; Nakashima, T. *J. Chem. Soc., Dalton Trans.* **1994**, 2339. (k) Matsumoto, N.; Mizuguchi, Y.; Mago, G.; Eguchi, S.; Miyasaka, H.; Nakashima, T.; Tuchagues, J. P. *Angew. Chem., Int. Ed. Engl.* **1997**, *36*, 1860.

(7) (a) Sunatsuki, Y.; Nakamura, M.; Matsumoto, N.; Kai, F. *Bull. Chem. Soc. Jpn.* **1997**, *70*, 1851. (b) Sunatsuki, Y.; Matsuo, T.; Nakamura, M.; Kai, F.; Matsumoto, N. *Bull. Chem. Soc. Jpn.* 1998, in press. (c) Sunatsuki, Y.; Hirata, R.; Motoda, Y.; Nakamura, M.; Matsumoto, N.; Kai, F. *Polyhedron* **1997**, *16*, 4105. (d) Sunatsuki, Y.; Shimada, H.; Mimura, M.; Kai, F.; Matsumoto, N. *Bull. Chem. Soc. Jpn.* **1998**, *71*, 167.

Table 1. Crystal Data for $[Mn(MeOH)L(OH)Zn(bpy)]_2 \cdot 4MeOH$ (**1**), $[Mn(MeOH)L(OH)Cu(bpy)]_2 \cdot 4MeOH$ (**2**), $[Mn(MeOH)L(OH)Ni(bpy)]_2 \cdot 4MeOH$ (**3**), and $[Mn(MeOH)L(OH)Mn(bpy)]_2 \cdot 2MeOH$ (**4**)[a]

	1	**2**	**3**	**4**
formula	$C_{68}H_{74}N_8O_{18}Mn_2Zn_2$	$C_{68}H_{74}N_8O_{18}Mn_2Cu_2$	$C_{68}H_{74}N_8O_{18}Mn_2Ni_2$	$C_{66}H_{66}N_8O_{16}Mn_4$
fw	1532.01	1528.34	1518.65	1447.04
space group	$P\bar{1}$ (no. 2)	$P2_1/n$ (no. 14)	$P\bar{1}$ (no. 2)	$P2_1/n$ (no. 14)
a, Å	12.367(3)	13.447(1)	12.358(3)	12.511(2)
b, Å	12.844(2)	12.670(2)	12.847(3)	21.129(3)
c, Å	12.262(2)	21.732(1)	12.315(3)	12.811(1)
α, deg	106.58(1)	90	106.63(2)	90
β, deg	117.89(1)	107.076(5)	118.71(1)	110.12(1)
γ, deg	78.57(2)	90	78.32(2)	90
V, Å^3	1645.0(6)	3539.3(5)	1638.2(7)	3179.8(7)
Z	1	2	1	2
ρ_{calcd}, g cm^{-3}	1.546	1.434	1.539	1.511
μ, cm^{-1}	11.75	10.15	10.22	8.52
R	4.0	5.9	6.7	6.7
R_w	3.4	4.9	3.6	7.2

[a] Reflection data were measured at 20 ± 1 °C. Mo Kα radiation (λ = 0.710 69 Å) was used. $R = \sum||F_o| - |F_c||/\sum|F_o|$, $R_w = [\sum w(|F_o| - |F_c|)^2/\sum w|F_o|^2]^{1/2}$, $w = 1/\sigma(F_o)^2$.

to the method in the literature.[8] The manganese(III) complex, $K[MnL(py)_2] \cdot py$, was prepared by a previously reported method.[7d]

$[Mn(MeOH)L(OH)Zn(bpy)]_2$ (1). To a solution of zinc(II) chloride (34 mg, 0.25 mmol) in 10 mL of methanol was added a solution of $K[MnL(py)_2] \cdot py$ (168 mg, 0.25 mmol) in 20 mL of methanol. The mixture was stirred for 1 h, and then a solution of bpy (39 mg, 0.25 mmol) in 10 mL of methanol was added to the mixture. The resulting solution was further stirred for 1 h and was left to stand for several days in a 50 mL sample bottle. During that time, brown crystals precipitated and were collected by suction filtration, washed with methanol and water, and then dried in vacuo. The crystals easily effloresced and were not soluble in solvents such as methanol, ethanol, DMF, and DMSO. Yield: 153 mg (24%). Anal. Calcd for **1**·MeOH, $C_{63}H_{54}N_8O_{13}Mn_2Zn_2$: C, 56.01; H, 4.02; N, 8.29%. Found: C, 55.61; H, 3.45; N, 8.60%. IR/cm^{-1}: 1598(ν_{CO}(amido)). UV−vis/nm: 531(sh) in the solid state. μ_{eff} per Mn_2Zn_2/μ_B: 6.82 at 300 K.

$[Mn(MeOH)L(OH)Cu(bpy)]_2$ (2). This compound was prepared in a way similar to that used for **1**, except for using copper(II) chloride dihydrate (86 mg, 0.5 mmol) instead of zinc(II) chloride. Dark brown crystals precipitated. Yield: 187 mg (29%). Anal. Calcd for **2**, $C_{62}H_{50}N_8O_{12}Mn_2Cu_2$: C, 55.74; H, 3.77; N, 8.39; Mn, 8.2; Cu, 9.5%. Found: C, 55.53; H, 3.40; N, 8.61; Mn, 8.1; Cu, 9.7%. IR/cm^{-1}: 1599(ν_{CO}(amido)). UV−vis/nm: 508(sh) in the solid state. μ_{eff} per Mn_2Cu_2/μ_B: 7.02 at 300 K.

$[Mn(MeOH)L(OH)Ni(bpy)]_2$ (3). This compound was prepared in a way similar to that used for **1**, except for using nickel(II) chloride hexahydrate (118 mg, 0.5 mmol) instead of zinc(II) chloride. Brown crystals precipitated. Yield: 181 mg (28%). Anal. Calcd for **3**, $C_{62}H_{50}N_8O_{12}Mn_2Ni_2$: C, 56.14; H, 3.80; N, 8.45; Mn, 8.3; Ni, 8.9%. Found: C, 56.15; H, 3.64; N, 8.59; Mn, 8.3; Ni, 8.8%. IR/cm^{-1}: 1603(ν_{CO}(amido)). UV−vis/nm: 582(sh), 1130(sh) in the solid state. μ_{eff} per Mn_2Ni_2/μ_B: 7.88 at 300 K.

$[Mn(MeOH)L(OH)Mn(bpy)]_2$ (4). This compound was prepared in a manner similar to that used for **1**, except for using manganese(II) chloride tetrahydrate (98 mg, 0.5 mmol) instead of zinc(II) chloride. Dark brown crystals precipitated. Yield: 114 mg (18%). Anal. Calcd for **4**·MeOH, $C_{63}H_{54}N_8O_{13}Mn_4$: C, 56.01; H, 4.02; N, 8.29; Mn, 16.3%. Found: C, 55.61; H, 3.45; N, 8.60; Mn, 17.0%. IR/cm^{-1}: 1596(ν_{CO}(amido)). UV−vis/nm: 576(sh) in solid state. μ_{eff} per Mn_2Mn_2/μ_B: 7.40 at 300 K.

Physical Measurements. Elemental analyses for C, H, and N were performed at the Elemental Analysis Service Center of Kyushu University. Elemental analyses for Cu, Ni, and Mn were made on a Hitachi 508 atomic absorption spectrophotometer. Infrared spectra were measured using the KBr disk method with a JASCO A-102 spectrophotometer. Electronic spectra were measured on a Hitachi U-4000 spectrophotometer. Magnetic susceptibilities under the applied magnetic field of 5000 G were measured with a MPMS5 SQUID susceptometer (Quantum Design Inc.) in the temperature range of 2−300 K. The calibrations were made with palladium and $[Ni(en)_3]S_2O_3$ (en = ethylenediamine).[9] Corrections were applied for the diamagnetism calculated from Pascal's constants.[10]

X-ray Data Collection, Reduction, and Structure Determination. Since all the single crystals, **1**−**4**, easily effloresce due to the elimination of the crystal solvents, each crystal was encapsulated into a Lindeman glass capillary with a small amount of the mother liquid. All crystallographic measurements were made on a Rigaku AFC-7R diffractometer with graphite monochromated Mo Kα radiation and a 12 kW rotating anode generator. The X-ray diffraction data were collected at a temperature of 20 ± 1 °C using the $\omega-2\theta$ scan technique at a scan speed of 16.0°/min (in ω) and the maximum 2θ value of 50°. The weak reflections ($I < 10.0\sigma(I)$) were rescanned (maximum of three scans), and the counts were accumulated to ensure good counting statistics. Stationary background counts were recorded on each side of the reflection. The ratio of peak counting time to background counting time was 2:1. The intensities of three representative reflections were measured after every 150 reflections, showing a good stability of the intensities. An empirical absorption correction based on the azimuthal scans of several reflections was applied. The data were corrected for Lorentz and polarization effects.

The structures were solved by direct methods[11] and expanded using Fourier techniques.[12] The non-hydrogen atoms were anisotropically refined. Hydrogen atoms at the ideal positions were included in the structure factor calculations but not refined. Full-matrix least-squares refinement based on the observed reflections ($I > 3.00\sigma(I)$) were employed, where the unweighted and weighted agreement factors of $R = \sum||F_o| - |F_c||/\sum|F_o|$ and $R_w = [\sum w(|F_o| - |F_c|)^2/\sum w|F_o|^2]^{1/2}$ were used. The weighting scheme was based on counting statistics. Neutral atomic scattering factors were taken from Cromer and Waber.[13] Anomalous dispersion effects were included in F_{calcd}; the values $\Delta f'$

(8) Anson, F. C.; Collins, T. J.; Richmond, T. G.; Santarsiero, B. D.; Toth, J. E.; Treco, B. G. R. T. *J. Am. Chem. Soc.* **1987**, *109*, 2974.
(9) Lindoy, L. F.; Katovic, V.; Busch, D. H. *J. Chem. Educ.* **1972**, *49*, 117.
(10) (a) Boudreaux, E. A.; Mulay, L. N. *Theory and Applications of Molecular Paramagnetism*; Wiley: New York, 1976; pp 491−495. (b) Earnshaw, A. *Introduction to Magnetochemistry*; Academic Press: New York, 1968.
(11) (a) Fan, H.-F. *SAPI91*, Structure Analysis Programs with Intelligent Control; Rigaku Corporation: Tokyo, Japan, 1991. (b) Debaerdemaeker, T.; Germain, G.; Main, P.; Refaat, L. S.; Tate, C.; Woolfson, M. M. *MULTAN88*; 1988.
(12) Beurskens, P. T.; Admiraal, G.; Beurskens, G.; Bosman, W. P.; Garcia-Granda, S.; Gould, R. O.; Smits, J. M. M.; Smykalla, C. *DIRDIF92*; The DIRDIF Program System, Technical Report of the Crystallography Laboratory; University of Nijmegen: The Netherlands, 1992.
(13) Cromer, D. T.; Waber, J. T. In *International Tables for X-ray Crystallography*; The Kynoch Press: Birmingham, England, 1974; Vol. IV, Table 2.2A.

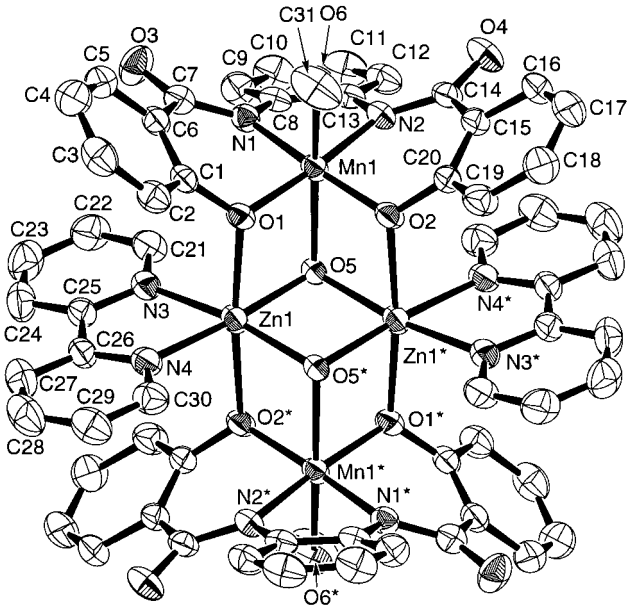

Figure 1. An ORTEP view of an incomplete double-cubane structure of $[Mn(MeOH)L(OH)Zn(bpy)]_2$ (**1**) with the atom numbering schemes, showing 30% probability ellipsoids. Hydrogen atoms are omitted for clarity.

and $\Delta f''$ were those of Creagh and McAuley.[14] All calculations were performed using the teXsan crystallographic software package from the Molecular Structure Corporation.[15] Crystal data and details of the structure determination for **1**−**4** are summarized in Table 1.

Results and Discussion

Synthesis and Characterization. The manganese(III) complex with a tetradentate ligand, $K[MnL(py)_2]\cdot py$, functions as an electronically mononegative ligand complex at the two phenoxo oxygen atoms. The ligand complex reacts with a metal(II) ion (M(II) = Zn, Cu, Ni, and Mn) and 2,2′-bipyridine as the terminal capping ligand in a 1:1:1 molar ratio in methanol to give a series of hetero metal complexes. The elemental analyses of C, H, N, and metal agreed with the formula $[Mn(MeOH)L(OH)M(bpy)]_2$. The complexes are sparingly soluble in common organic solvents and water. These complexes showed infrared absorption bands assignable to $\nu_{C=O}$(amido) vibrations at 1603−1596 cm^{-1}.[16] The diffuse reflectance spectra were measured in the region of 300−1200 nm. The precursor Mn(III) complex shows a shoulder band at 499 nm attributable to a d−d band of Mn(III). This band shifts to a longer wavelength in the tetranuclear complexes **1**−**4** (508−582 nm). In addition to this band, the spectrum of **3** showed another shoulder band at 1130 nm attributable to a d−d band of Ni(II).

X-ray Crystal Structures of $[Mn(MeOH)L(OH)M(bpy)]_2$ (M = Zn(II), Cu(II), Ni(II), and Mn(II)). **2** and **4** crystallize in the monoclinic space group $P2_1/n$ with $Z = 2$. **1** and **3** are isomorphous to each other and crystallize in the triclinic space group $P\bar{1}$ with $Z = 1$. The ORTEP views of **1**−**4** with the atom numbering schemes are shown in Figures 1−4, respectively, in which the same atom numbering scheme is adapted for all the complexes. The selected bond distances and angles with their estimated standard deviations are summarized in Table 2.

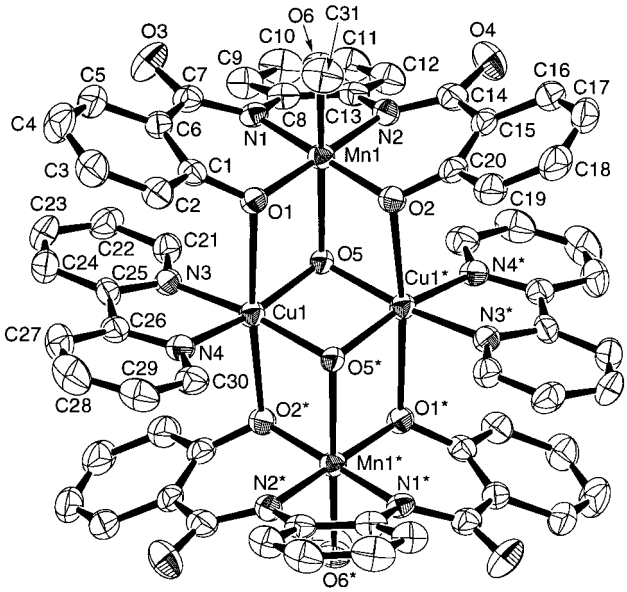

Figure 2. An ORTEP view of an incomplete double-cubane structure of $[Mn(MeOH)L(OH)Cu(bpy)]_2$ (**2**) with the atom numbering schemes, showing 30% probability ellipsoids. Hydrogen atoms are omitted for clarity.

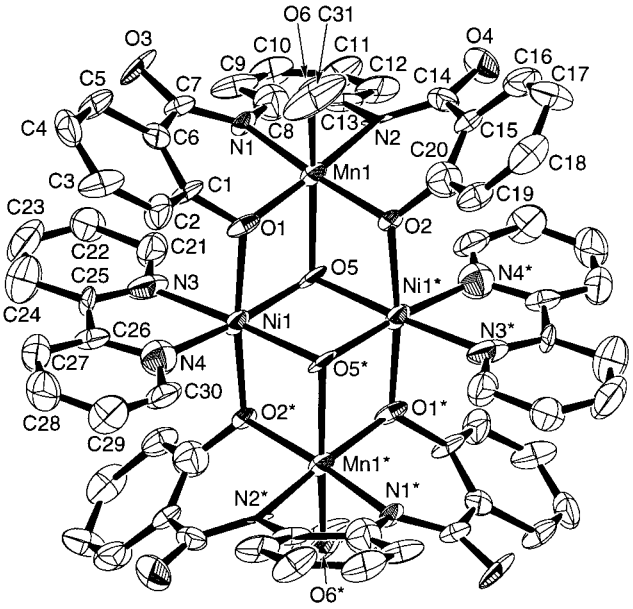

Figure 3. An ORTEP view of an incomplete double-cubane structure of $[Mn(MeOH)L(OH)Ni(bpy)]_2$ (**3**) with the atom numbering schemes, showing 30% probability ellipsoids. Hydrogen atoms are omitted for clarity.

All the complexes assume a tetranuclear incomplete double-cubane structure with a $[Mn_2M_2O_6]$ core, and the molecule has an inversion center. In the incomplete double-cubane structure, two metal(II) ions are bridged by two hydroxo groups to form a planar dinuclear moiety bridged by di-μ-hydroxo groups $[(bpy)M(OH)_2M(bpy)]^{2+}$ and the dinuclear moiety is sandwiched between two Mn(III) ligand complexes $[MnL(MeOH)]^-$. The Mn(III) ion and dinuclear M(II) moiety are triply bridged by one hydroxo ion of the dinuclear moiety and two phenoxo oxygen atoms of the Mn(III) ligand complex.

Each Mn(III) ion assumes a square bipyramidal coordination geometry with the N_2O_4 donor atoms of a tetradentate ligand, a methanol molecule, and a hydroxo oxygen of $[(bpy)M(OH)_2M(bpy)]^{2+}$. The two axial sites of the Mn(III) ion are occupied by O(6) of a methanol molecule and a hydroxo oxygen

(14) Creagh, D. C.; McAuley, W. J. In *International Tables for Crystallography*; Wilson, A. J. C., Ed.; Kluwer Academic Publishers: Boston, MA, 1992; Vol. C, Table 4.2.6.8, pp 219−222.
(15) *teXsan*: *Crystal Structure Analysis Package*; Molecular Structure Corporation: The Woodlands, TX, 1985 and 1992.
(16) Nakamoto, K. *Infrared and Raman Spectra of Inorganic and Coordination Compounds*, 4th ed.; John Wiley & Sons: New York, 1986.

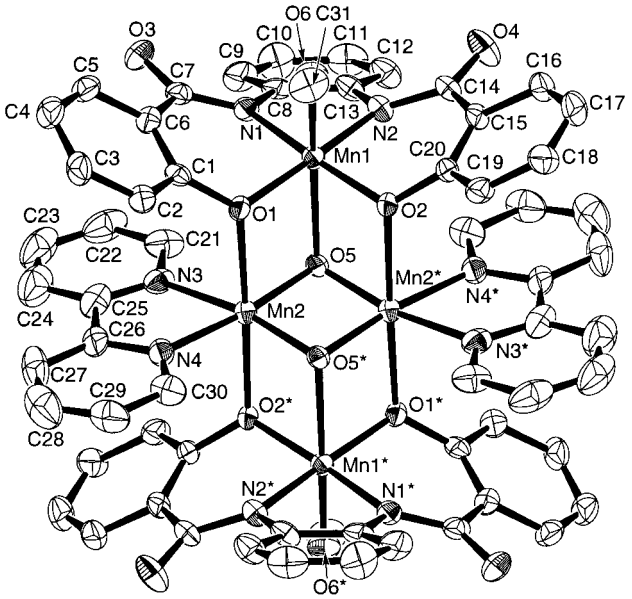

Figure 4. An ORTEP view of an incomplete double-cubane structure of $[Mn(MeOH)L(OH)Mn(bpy)]_2$ (**4**) with the atom numbering schemes, showing 30% probability ellipsoids. Hydrogen atoms are omitted for clarity.

Table 2. Relevant Bond Distances (Å) and Bond Angles (deg) of Incomplete Double-Cubane Complexes $[Mn(MeOH)L(OH)Zn(bpy)]_2 \cdot 4MeOH$ (**1**), $[Mn(MeOH)L(OH)Cu(bpy)]_2 \cdot 4MeOH$ (**2**), $[Mn(MeOH)L(OH)Ni(bpy)]_2 \cdot 4MeOH$ (**3**), and $[Mn(MeOH)L(OH)Mn(bpy)]_2 \cdot 2MeOH$ (**4**)

	1	**2**	**3**	**4**
		Distances (Å)		
Mn(1)−N(1)	1.945(3)	1.939(6)	1.96(1)	1.946(8)
Mn(1)−N(2)	1.947(3)	1.951(6)	1.95(1)	1.933(8)
Mn(1)−O(1)	1.927(2)	1.883(4)	1.92(1)	1.918(6)
Mn(1)−O(2)	1.901(2)	1.888(5)	1.950(9)	1.921(6)
Mn(1)−O(5)	2.314(3)	2.403(4)	2.34(1)	2.353(6)
Mn(1)−O(6)	2.289(3)	2.283(5)	2.28(1)	2.233(7)
M(1)−O(5)	2.073(2)	1.980(4)	2.02(1)	1.890(6)
M(1)−O(5)[a]	2.055(2)	1.969(4)	2.09(1)	1.889(6)
M(1)−O(1)	2.228(3)	2.560(4)	2.15 (1)	2.269(6)
M(1)−O(2)[a]	2.280(3)	2.545(5)	2.157(10)	2.315(6)
M(1)···M(1)[a]	3.072(1)	2.954(2)	3.112(4)	2.744(3)
M(1)···Mn(1)	3.2497(8)	3.367(1)	3.203(3)	3.211(2)
M(1)[a]···Mn(1)	3.2766(9)	3.364(1)	3.195(3)	3.247(2)
Mn(1)···Mn(1)[a]	5.758(2)	6.048(2)	5.590(4)	5.846(3)
		Angles (deg)		
O(5)−M(1)−O(5)[a]	83.8(1)	83.1(2)	81.9(5)	86.9(3)
M(1)−O(5)−M(1)[a]	96.2(1)	96.9(2)	98.1(5)	93.1(3)
M(1)−O(5)−Mn(1)	95.4(1)	99.9(2)	94.2(5)	97.8(3)
M(1)−O(5)−Mn(1)	97.0(1)	100.1(2)	92.1(5)	99.3(3)
M(1)−O(1)−Mn(1)	102.7(1)	97.3(2)	103.7(4)	99.8(3)
M(1)[a]−O(2)−Mn(1)	102.8(1)	97.6(2)	102.0(5)	99.7(3)

[a] Refers to the equivalent position $-x, -y, -z$.

atom O(5). The Mn−O(6) (methanol) distances for **1**−**4** are in the range of 2.233(7)−2.289(3) Å and the Mn−O(5) distances (hydroxo ion) are in the range of 2.314(3)−2.403(4) Å. The equatorial coordination sites are occupied by the N_2O_2 donor atoms consisting of two amido nitrogens and two phenoxo oxygen atoms of the tetradentate ligand. The Mn−N distances of the tetranuclear complexes (**1**−**4**) are nearly equal to each other (1.938(8)−1.96(1) Å) and are shorter than that in the precursor ligand complex $K[MnL(py)_2] \cdot py$.[7d] The Mn−O distance of **2** is equal to that of the precursor ligand complex, but the Mn−O distance of the other tetranuclear complexes (**1**, **3**, and **4**) are longer than that of the ligand complex.

Each metal(II) ion assumes a similar square bipyramidal coordination geometry with the N_2O_4 donor atoms consisting of a bpy, two hydroxo, and two phenoxo oxygen atoms. The two axial coordination sites are occupied by a phenoxo oxygen atom O(1) of a Mn(III) ligand complex at the upper part and a phenoxo oxygen atom O(2)* of another Mn(III) complex at the lower part. The M(II)−O(1) and M(II)−O(2)* distances distribute from the longest one of 2.560(4) Å for Cu (**2**) to the shortest one of 2.15(1) Å for Ni (**3**), depending on the metal(II) ion. The elongation of the axial coordination found in Cu (Cu−O(1) = 2.560(4) Å and Cu−O(2)* = 2.545(5) Å) is ascribed to the Jahn−Teller effect.

The present incomplete double-cubane complexes contain a dinuclear structure bridged by a di-μ-hydroxo moiety $[(bpy)M(OH)_2M(bpy)]^{2+}$. Since the dinuclear metal(II) complexes bridged by the di-μ-hydroxo moiety have been extensively studied with the aim to elucidate the magnetic mechanism between the magnetic centers[17] and as the functional compounds to fix atmospheric carbon dioxide,[18] it would be interesting to compare the structural parameters with those of the already reported complexes.

The bond distances of **2** ($\langle Cu-N \rangle = 1.993$ Å and $\langle Cu-O \rangle = 1.975$ Å) can be compared with the corresponding values reported for $[(bpy)Cu(OH)_2Cu(bpy)]X_n$, ($\langle Cu-N \rangle = 1.98-2.00$ Å and $\langle Cu-O \rangle = 1.91-1.95$ Å).[17] The Cu···Cu separation (2.953(3) Å) is longer than the Cu···Cu separation (2.847−2.893 Å) found in $[(bpy)Cu(OH)_2Cu(bpy)]X_n$. The bond angle Cu(1)−O(5)−Cu(1)* (96.9(2)°) lies in the range of that for $[(bpy)Cu(OH)_2Cu(bpy)]X_n$ (Cu−O(5)−Cu = 95.6−97.0°).

Kitajima et al. reported the synthesis, crystal structure, and fixation of atmospheric carbon dioxide for a series of dinuclear complexes bridged by a di-μ-hydroxo moiety $[L'M(OH)_2ML']$ (M = Mn(II), Fe(II), Co(II), Ni(II), and Cu(II); L′ = hydrotris(3,5-di-*iso*-propyl-1-pyrazoyl)borate).[18] The bridging angles of M−O−M are substantially larger than those of our complexes; the angles of Kitajima's complexes are in the range of 98.6(2)−106.1(3)°, while those of our complexes are in the range of 93.1(3)−98.1(5)°. The Ni−O(5) and Ni−O(5)* bond distances for **3** are longer and the Ni(1)···Ni(1)* separation is shorter than those of $[L'Ni(OH)_2NiL']$. Special attention should be paid to the Mn(II) complex, where the Mn(II) ion in $[L'Mn(OH)_2MnL']$ is confirmed to be in a high-spin state. The distances of Mn−O(5) = 1.890(6) Å and Mn−O(5)* = 1.889(6) Å for **4** are shorter than those of $[L'Mn(OH)_2MnL']$ (2.0989(5), 2.094(4) Å). The Mn(2)···Mn(2)* distance and the bridging angle Mn−O−Mn are 2.744(3) Å and 93.1(3)° for **4** and 3.314(1) Å and 104.8(2)° for $[L'Mn(OH)_2MnL']$, respectively. Furthermore, the axial Mn−O distances of 2.315(6) and 2.269(6) Å for **4** are fairly short. The structural features were in accord with those

(17) (a) Hodgson, D. J. In *Magneto-Structural Correlations in Exchange Coupled Systems*; Willet, R. D., Gatteschi, D., Kahn, O., Eds.; Reidel: Dordrecht, The Netherlands, 1985; p 497. (b) McGregor, K. T.; Watkins, N. T.; Lewis, D. L.; Drake, R. F.; Hodgson, D. J.; Hatfield, W. E. *Inorg. Nucl. Chem. Lett.* **1973**, *9*, 423. (c) Barnes, J. A.; Hodgson, D. J.; Hatfield, W. E. *Inorg. Chem.* **1972**, *11*, 144. (d) Cairns, C. J.; Busch, D. H. *Coord. Chem. Rev.* **1986**, *69*, 1. (e) Casey, A. T.; Hoskins, B. F.; Whillans, F. D. *J. Chem. Soc., Chem. Commun.* **1970**, 1593. (f) Hoskins, B. F.; Whillans, F. D. *J. Chem. Soc., Dalton Trans.* **1975**, 1267. (g) Toofan, M.; Boushehri, A.; Haque, M. *J. Chem. Soc., Dalton Trans*. **1976**, 217. (h) Handa, M.; Idehara, T.; Nakano, K.; Kasuga, K.; Mikuriya, M.; Matsumoto, N.; Kodera, M.; Kida, S. *Bull. Chem. Soc. Jpn.* **1992**, *65*, 3241.

(18) (a) Kitajima, N.; Hikichi, S.; Tanaka, M.; Moro-oka, Y. *J. Am. Chem. Soc.* **1993**, *115*, 5496. (b) Hikichi, S.; Komatsuzaki, H.; Kitajima, N.; Akita, M.; Mukai, M.; Kitagawa, T.; Moro-oka, Y. *Inorg. Chem*. **1997**, *36*, 266. (c) Kitajima, N.; Singh, U. P.; Amagi, H.; Osawa, M.; Moro-oka, Y. *J. Am. Chem. Soc*. **1991**, *113*, 7757.

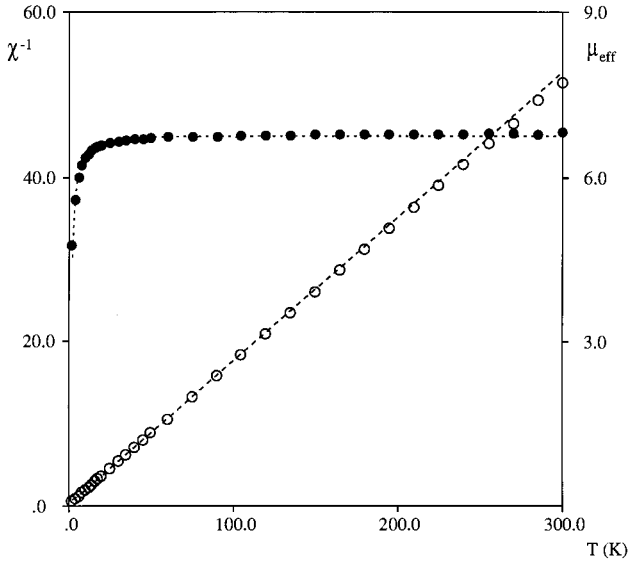

Figure 5. Temperature dependence of the inverse of the magnetic susceptibility and effective magnetic moment per tetranuclear molecule for $[Mn(MeOH)L(OH)Zn(bpy)]_2$ (**1**). The solid and dotted lines represent the best-fit calculated curves using the parameters of $g_{Mn} = 1.96$, $D_{Mn} = -4.7$ cm^{-1}.

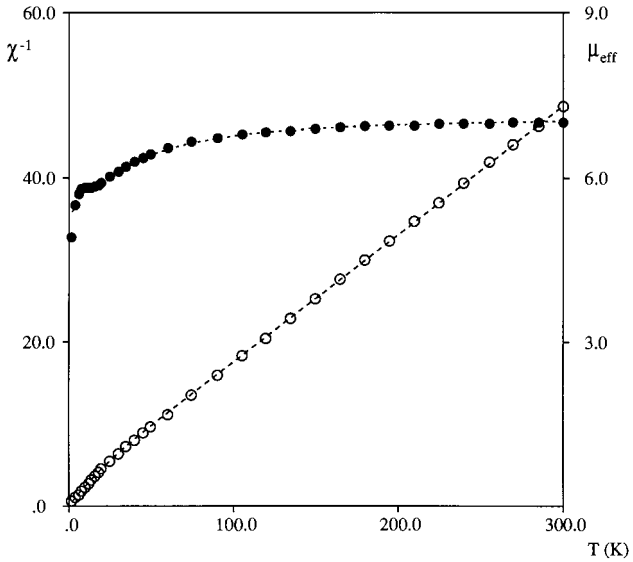

Figure 6. Temperature dependence of the inverse of the magnetic susceptibility and effective magnetic moment per tetranuclear molecule for $[Mn(MeOH)L(OH)Cu(bpy)]_2$ (**2**). The solid and dotted lines represent the best-fit calculated curves using the parameters of $g_{Mn} = 1.91$, $g_{Cu} = 2.39$, $J = -4.5$ cm^{-1}, $J' = -8.1$ cm^{-1}, and $D_{Mn} = -4.9$ cm^{-1}.

of the Mn(II) ion in **4** in a low-spin state, as confirmed by the magnetic measurements to be described later.

Effect of the Metal Ion of the Ligand Complex on Multinuclear Structure. The double-cubane structure derived from the Mn(III) ligand complex is distinctly different from the dinuclear and cyclic, tetranuclear structures derived from the ligand complexes of copper(II) and nickel(II) with the same ligand. It is proper to consider why such a different structure can be produced by the effect of a metal ion. Both in the present incomplete double-cubane structure and the multinuclear structure derived from the Cu(II) ligand complex, the Mn(III) and Cu(II) ligand complexes act as bidentate "ligand complexes" at the two phenoxo-oxygen atoms. The two phenoxo oxygen atoms of the Mn(III) ligand complex coordinate as an axial ligand to two independent metal(II) ions, while those of the Cu(II) complex coordinate as an equatorial bidentate ligand to a metal(II) ion. Furthermore, the Mn(III) complex functions not only as a bidentate ligand but also accepts a donor atom at the axial coordination site, while the Cu(II) complex with the strong donating tetradentate ligand has no ability to accept donor atoms at the axial site. The Mn(III) complex is a mononegative ion, while the Cu(II) complex is a dinegative ion. The dinegative Cu(II) complex reacted with a metal(II) and a neutral capping ligand to form an electrically neutral dinuclear complex. This dinuclear species would be stable even in solution as confirmed by the solution chemistry.[7c] On the other hand, the Mn(III) complex is a mononegative ion, and as a result, two Mn(III) complexes reacted with a dipositive dinuclear moiety $[(bpy)M(OH)_2M(bpy)]^{2+}$ to form an electrically neutral tetranuclear species $[Mn(MeOH)L(OH)M(bpy)]_2$. The metal ion in this ligand complex system affects the bridging mode, coordination number, and electronic charge. These factors cooperatively work to determine the resulting multinuclear structure.

Magnetic Properties. The magnetic susceptibilities under the external magnetic field of 5000 G were measured in the temperature range of 2−300 K. The magnetic behaviors of **1**−**4** are shown in Figures 5−8, respectively, as $1/\chi_M$ vs T and μ_{eff} vs T plots, where χ_M is the magnetic susceptibility per tetranuclear unit and μ_{eff} is the effective magnetic moment.

The effective magnetic moments at room temperature, with the spin-only values in parentheses, and the spin-system are given in Table 3, where the spin-only values were calculated using the equations $\mu_{so} = (2\mu_{Mn}^2 + 2\mu_M^2)^{1/2}$; $\mu_{Mn} = [2S_{Mn}(S_{Mn} + 1)]^{1/2}$, $S_{Mn} = 2$; $\mu_M = [2S_M(S_M + 1)]^{1/2}$, $S_M = 0$, 1/2, 1, and 1/2 for Zn(II), Cu(II), Ni(II), and Mn(II), respectively. These effective magnetic moments at room temperature are compatible with the corresponding spin-only values assuming no magnetic interaction, indicating that all the Mn(III), d^4, ions in these complexes are in a high-spin state, $S = 2$, and the metal(II) ions except for Mn(II) in **4** are in high-spin states. It is noteworthy that the Mn(II), d^5, ions in **4** are in a low-spin state, $S = 1/2$. Low-spin Mn(II) complexes are quite rare,[19] although a number of di- and tetranuclear manganese complexes bridged

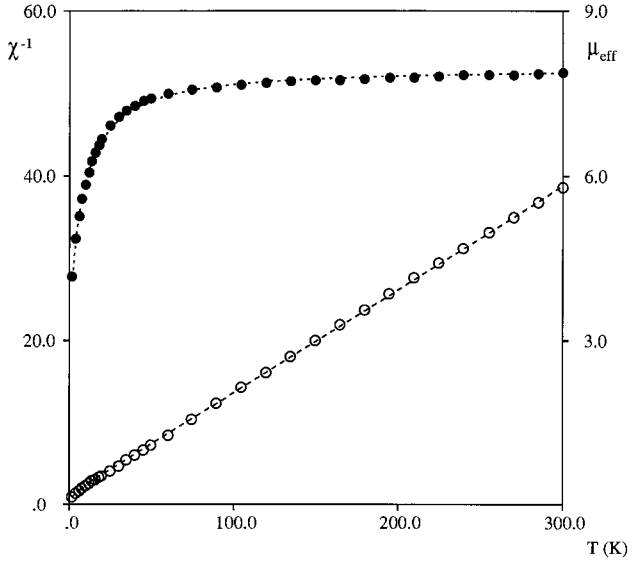

Figure 7. Temperature dependence of the inverse of the magnetic susceptibility and effective magnetic moment per tetranuclear molecule for $[Mn(MeOH)L(OH)Ni(bpy)]_2$ (**3**). The solid and dotted lines represent the best-fit calculated curves using the parameters of $g_{Mn} = 1.97$, $g_{Ni} = 2.23$, $J = -1.5$ cm^{-1}, $J' = -2.6$ cm^{-1}, and $D_{Mn} = -5.5$ cm^{-1}.

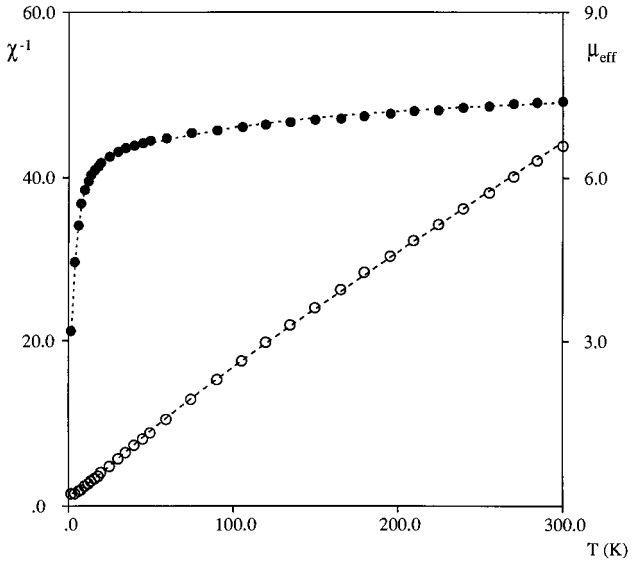

Figure 8. Temperature dependence of the inverse of the magnetic susceptibility and effective magnetic moment per tetranuclear molecule for $[Mn(MeOH)L(OH)Mn(bpy)]_2$ (**4**). The solid and dotted lines represent the best-fit calculated curves using the parameters of $g_{Mn} = 1.95$, $g_{Mn(II)} = 2.29$, $J = -3.5$ cm^{-1}, $J' = -14.1$ cm^{-1}, and $D_{Mn} = -12.0$ cm^{-1}.

by a di-μ-oxo, di-μ-hydroxo, or μ-oxo-μ-hydroxo moiety have been prepared and extensively studied as model compounds of redox-active enzymes, manganese catalysts, and photosystem II.[20]

The magnetic behavior of $[Mn(MeOH)L(OH)Zn(bpy)]_2$ **1** is well reproduced by two noninteracting Mn(III) spin centers, including zero-field splitting, with $g_{Mn} = 1.96$ and $D_{Mn} = -4.7$ cm^{-1} (see Figure 5). We also fitted the data allowing for an exchange interaction between the two Mn(III) ions, i.e., using the following spin Hamiltonian (1).

$$\mathbf{H} = g_{Mn}\beta(\mathbf{S}_1 + \mathbf{S}_3)\cdot H - 2J''(\mathbf{S}_1\cdot\mathbf{S}_3) + D_{Mn}[\mathbf{S}_{1z}{}^2 + \mathbf{S}_{3z}{}^2] \quad (1)$$

The obtained J'' value of -0.06 cm^{-1} (g_{Mn} and D_{Mn} remain essentially constant) showed no real improvements in the fit. This shows that the Mn(III)−Mn(III) diagonal interaction is negligible; therefore, it will be neglected in the interpretation of the magnetic properties of **2**−**4** (vide infra).

For **2**−**4**, the effective magnetic moment μ_{eff} decreases slowly upon lowering the temperature, thus suggesting dominant antiferromagnetic interactions. In an attempt to reproduce the experimental susceptibility data of **2**−**4**, we used the following zero-field Hamiltonian (eq 2) based on the rhombus spin coupling model sketched in Scheme 3 with spin (S_1, S_2, S_3, S_4) = (2, S_M, 2, S_M), and $S_M = 1/2$ for **2** and **4**, and $S_M = 1$ for **3**:

$$\mathbf{H} = -2J(\mathbf{S}_1\cdot\mathbf{S}_2 + \mathbf{S}_2\cdot\mathbf{S}_3 + \mathbf{S}_3\cdot\mathbf{S}_4 + \mathbf{S}_4\cdot\mathbf{S}_1) - 2J'(\mathbf{S}_2\cdot\mathbf{S}_4) \quad (2)$$

where J and J' are the Mn(III)−M(II) and M(II)−M(II) Heisenberg coupling constants, respectively. No Mn(III)−Mn(III) diagonal interaction has been included, as this is expected to be very weak due to the long Mn···Mn distance (i.e., 5.758(2) Å for **4**) and the absence of any bridging ligand. This assumption is also supported by the analysis of the magnetic data of **1** showing the absence of coupling between the two Mn(III) ions. The eigenvalues of the Hamiltonian (eq 2) can be derived using the vector coupling method of Kambe:[21]

$$E(S, S', S'') = -J[S(S+1) - S'(S'+1) - S''(S''+1)] - J'S''(S''+1) \quad (3)$$

where $S = S' + S''$ is the total spin and $S' = S_1 + S_3$, $S'' = S_2 + S_4$. A total of 18 spin states (S, S', S'') with S values ranging from 0 to 5 are obtained for **2** and **4**, while 37 spin states with S values from 0 to 6 are obtained for **3**. The magnetic susceptibility per tetranuclear complex is given by the following Van-Vleck eq 4:[22]

$$\chi_M = [Ng^2\beta^2\sum_S\sum_{S'}\sum_{S''}S(S+1)(2S+1)\exp(-E(S,S',S'')/kT)]/[3kT\sum_S\sum_{S'}\sum_{S''}(2S+1)/\exp(-E(S,S',S'')/kT)] \quad (4)$$

where N is Avogadro's number, k is the Boltzmann constant, g is the average g factor, and the sum is extended to all spin states of the tetramer; S' varies by an integer value from 0 to 4, S'' from 0 to $2S_2$, and S from $|S' - S''|$ to $S' + S''$. However, this theoretical curve failed to adequately reproduce the low-temperature magnetic data, in particular, the sharp drop of μ_{eff} below 25 K. This is mainly due to the neglect of the zero-field splitting, which for the Mn(III) ions may be in the range of a few wavenumber, the same order of magnitude of the coupling constants J and J' evaluated by a fit of the experimental data above 25 K. We thus considered a more complete Hamiltonian including a zero-field splitting term for the Mn(III) ions and by considering two distinct g factors for the Mn(III) and M(II) ions:

$$\mathbf{H} = g_{Mn}\beta(\mathbf{S}_1 + \mathbf{S}_3)\cdot H + g_M\beta(\mathbf{S}_2 + \mathbf{S}_4)\cdot H - 2J(\mathbf{S}_1\cdot\mathbf{S}_2 + \mathbf{S}_2\cdot\mathbf{S}_3 + \mathbf{S}_3\cdot\mathbf{S}_4 + \mathbf{S}_4\cdot\mathbf{S}_1) - 2J'(\mathbf{S}_2\cdot\mathbf{S}_4) + D_{Mn}[\mathbf{S}_{1z}{}^2 + \mathbf{S}_{3z}{}^2] \quad (5)$$

in which H is the applied field, g_{Mn} and g_M are the g factors of Mn(III) and M(II), respectively, and D is the zero-field splitting parameter of Mn(III). The zero-field splitting for the Ni(II) ions in **3** and the effect of monomeric impurities or intermolecular interactions were not included in order to avoid overparametrization. The magnetic susceptibility at each temperature point was calculated using the following theoretical equation.[22]

$$\chi = M/H = [N\sum_i(-dE_i/dH)\exp(-E_i/kT)]/[H\sum_i\exp(-E_i/kT)] \quad (6)$$

The energy levels of the tetramers, E_i, are evaluated by diagonalizing the Hamiltonian matrix (with dimensions 100 × 100 for **2** and **4** and 225 × 225 for **3**) in the uncoupled spin functions basis set. The magnetic data of **2**−**4** over the entire

(19) (a) Gouzerh, P.; Jeanin, Y.; Rocchiccioli-Deltcheff, C.; Valentini, F. *J. Coord. Chem.* **1979**, *6*, 221. (b) Cotton, F. A.; Wilkinson, G. *Advanced Inorganic Chemistry*, 5th ed.; Wiley: New York, 1988.
(20) (a) Boucher, L. J.; Goe, C. G. *Inorg. Chem.* **1975**, *14*, 1289. (b) Boucher, L. J.; Goe, C. G. *Inorg. Chem.* **1976**, *15*, 1334. (c) Sawyer, D. T.; Bodini, M. E. *J. Am. Chem. Soc.* **1975**, *97*, 6588. (d) Pecoraro, V. L.; Baldwin, M. J.; Gelasco, A. *Chem. Rev.* **1994**, *94*, 807. (e) Dismukes, G. C. *Chem. Rev.* **1996**, *96*, 2909. (f) Yachandra, V. K.; Sauer, K.; Klein, M. P. *Chem. Rev.* **1996**, *96*, 2927. (g) Wieghardt, K. *Angew. Chem., Int. Ed. Engl.* **1989**, *28*, 1153.
(21) Kambe, K. *J. Phys. Soc. Jpn.* **1950**, *5*, 48.
(22) Van-Vleck, J. H. *The Theory of Electric and Magnetic Susceptibilities*; Oxford University Press: London, 1932.

Table 3. Effective Magnetic Moments at 300 K (Spin-Only Values in Parentheses), Spin-System,[a] and the Fitting Parameters

complex	μ_{eff}/μ_B	μ_{so}/μ_B[b]	spin-system (2, S_M, 2, S_M)	J/cm^{-1}, J'/cm^{-1}, D/cm^{-1}
1 [Mn(III), Zn(II)]$_2$	6.82	6.92	(2, 0, 2, 0)	
2 [Mn(III), Cu(II)]$_2$	7.01	7.34	(2, 1/2, 2, 1/2)	−4.5, −8.1, −4.9
3 [Mn(III), Ni(II)]$_2$	7.88	8.00	(2, 1, 2, 1)	−1.5, −2.6, −5.5
4 [Mn(III), Mn(II)]$_2$	7.40	7.34	(2, 1/2, 2, 1/2)	−3.5, −14.1, −12.0

[a] See Scheme 3. [b] The effective magnetic moment per tetranuclear molecule at 300 K for **1**−**4**. The spin-only value is calculated by the equation $\mu_{so} = (2\mu_{Mn}^2 + 2\mu_M^2)^{1/2}$; $\mu_{Mn} = [2S_{Mn}(S_{Mn} + 1)]^{1/2}$, $S_{Mn} = 2$; $\mu_M = [2S_M(S_M + 1)]^{1/2}$, $S_M = 0$, 1/2, 1, and 1/2 for Zn(II), Cu(II), Ni(II), and Mn(II), respectively.

Scheme 3

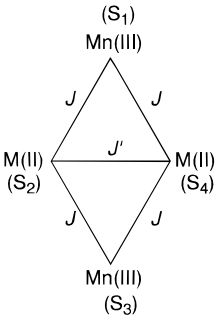

range of temperatures were well reproduced with the Hamiltonian (5) in Figures 6−8, and the calculated best-fit parameters are $g_{Mn} = 1.91$, $g_{Cu} = 2.39$, $J = -4.5$ cm^{-1}, $J' = -8.1$ cm^{-1}, and $D_{Mn} = -4.9$ cm^{-1} for **2**; $g_{Mn} = 1.97$, $g_{Ni} = 2.23$, $J = -1.5$ cm^{-1}, $J' = -2.6$ cm^{-1}, and $D_{Mn} = -5.5$ cm^{-1} for **3**; and $g_{Mn} = 1.95$, $g_{Mn(II)} = 2.29$, $J = -3.5$ cm^{-1}, $J' = -14.1$ cm^{-1}, and $D_{Mn} = -12.0$ cm^{-1} for **4**. Note that the calculated zero-field splitting parameters in **2** and **3** are in the range observed for other Mn(III) complexes[23] while they are larger in **4**, probably because it accounts for the effects of anisotropic couplings or intermolecular interactions. Moreover, these values are of the same order of magnitude of the coupling constants, thus explaining the failure of the Hamiltonian (2) in reproducing the experimental data.

Spin Frustration. Compounds **2**−**4** have ground states that result from spin frustration,[24a] and their spin structure is topologically equivalent to some magnetically characterized manganese and iron tetramers.[24b] This can be better analyzed if we consider the eigenstates of the Hamiltonian (2) by neglecting the zero-field splitting and the field-dependent terms. Complex **2** has a (3, 4, 1) ground state which results from an antiferromagnetic alignment of the vector-coupled terms $S' = 4$ and $S'' = 1$. Such a spin coupling is determined by the Mn(III)−Cu(II) antiferromagnetic interaction J, which orientates both Cu(II) spins antiparallel to those on the Mn(III) ions as shown in Scheme 4. The net results of this spin alignment are that the spins of the two Cu(II) ions tend to be parallel even if the Cu(II)−Cu(II) interaction J' is antiferromagnetic. This is possible, however, only if J' is not strong enough to overcome J. Figure 9 illustrates a plot of the lowest eigenvalues of the Hamiltonian (2) with $S_M = 1/2$ as a function of the ratio J'/J calculated for $J < 0$ and $J' < 0$ (i.e., when both interactions are antiferromagnetic). It can be seen that the ground state is (3, 4, 1) for $J'/J < 5$ and is a mixture of spin states (S, S, 0) with $S = 0-4$ for $J'/J > 5$. In the present case, the two interactions are both antiferromagnetic with $J'/J \approx 0.7$ and the ground state is (3, 4, 1) with the first excited state (2, 3, 1) at 9.0 cm^{-1} and the (1, 2, 1) state at 18.0 cm^{-1}. This accounts for the anomalous plateau of the magnetic moment at low temperature followed by a further decrease below 8 K (see Figure 6). Indeed, such an energy level ordering would cause a low-temperature increase in the magnetic moment (to a spin-only limit value of 6.93μ_B) in the absence of the zero-field splitting, as confirmed by a simulation run with the same best-fit values except for D_{Mn}, which is set to zero. It is noteworthy that the fit of the magnetic data below 100 K for **2** is not very sensible for the value of J', at least as long as J' remains more positive than about (2−3)J,

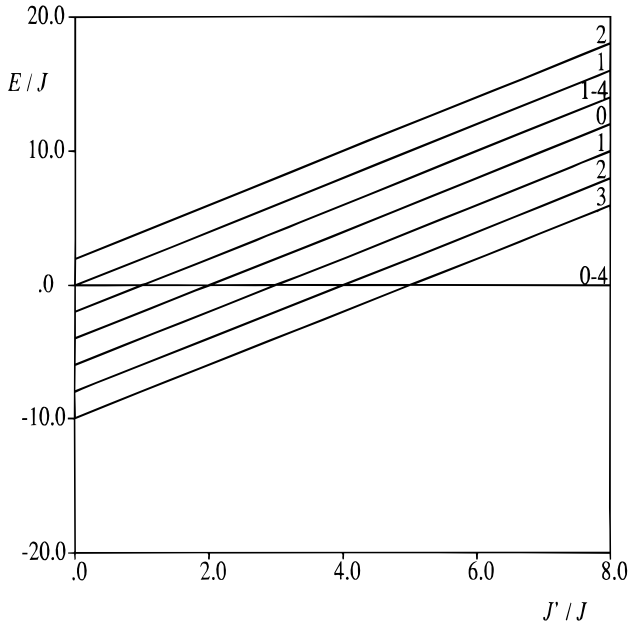

Figure 9. Plot of the lowest eigenvalues of the Hamiltonian (eq 2) for the (2, 1/2, 2, 1/2) spin system, calculated for $J < 0$ and $J' < 0$, as function of the J'/J ratio. Numbers on the lines correspond to the total spin values.

Scheme 4

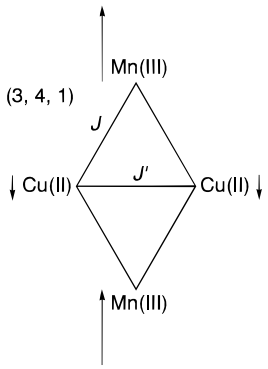

(23) Kennedy, B. J.; Murray, K. S. *Inorg. Chem.* **1985**, *24*, 1552.
(24) (a) McCusker, J. K.; Schmitt, E. A.; Hendrickson, D. N. In *Magnetic Molecular Materials*; Gatteschi, D., Kahn, O., Miller, J. S., Palacio, F., Eds.; NATO ASI Series E; Kluwer Academic: Dordrecht, The Netherlands, 1991; Vol. 198, p 297. (b) Vincent, J. B.; Christmas, C.; Chang, H.-R.; Li, Q.; Boyd, P. D. W.; Huffman, J. C.; Hendrickson, D. N.; Christou, G. *J. Am. Chem. Soc.* **1989**, *111*, 2086. McCusker, J. K.; Vincent, J. B.; Schmitt, E. A.; Mino, M. L.; Shin, K.; Coggin, D. K.; Hagen, P. M.; Huffman, J. C.; Cristou, G.; Hendrickson, D. N. *J. Am. Chem. Soc.* **1991**, *113*, 3013.

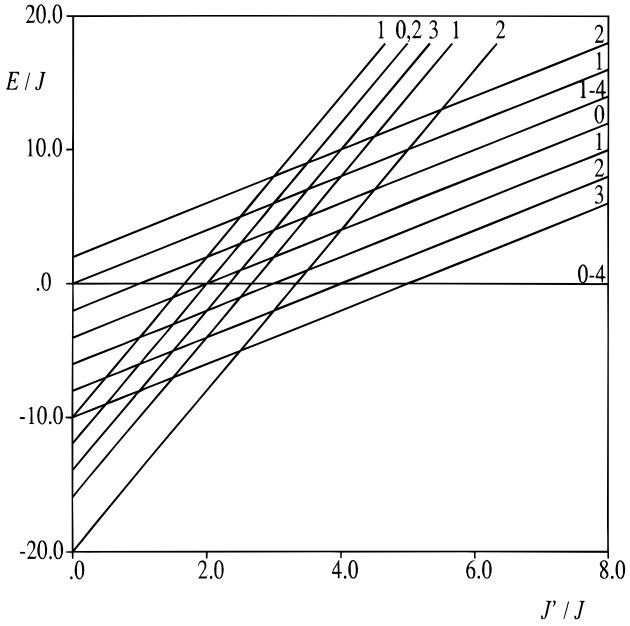

Figure 10. Plot of the lowest eigenvalues of the Hamiltonian (eq 2) for the (2, 1, 2, 1) spin system, calculated for $J < 0$ and $J' < 0$, as function of the J'/J ratio. Numbers on the lines correspond to the total spin values.

i.e., $J' < -10$ cm^{-1}. This is because the relative energies of the ground and the first excited states depend only on J and not J' for $J'/J < 2-3$, as illustrated by Figure 9.

An analogous situation is found in **4** whose ground state is still (3, 4, 1). However, in this case, the ratio J'/J is ca. 4 and there are several degenerate low-lying spin states (S, S, 0) with $S = 0-4$, within 7 cm^{-1}. The ground state of **3** is (2, 4, 2) resulting again from an antiferromagnetic alignment of the vector-coupled terms $S' = 4$ and $S'' = 2$, determined by the Mn(III)−Ni(II) antiferromagnetic interaction J, which orientates both Ni(II) spins antiparallel to those on the Mn(III) ions and frustrates the antiferromagnetic Ni(II)−Ni(II) interaction. Figure 10 is a plot of the lowest eigenvalues of the Hamiltonian (2) with $S_M = 1$ as a function of the ratio J'/J (calculated for $J < 0$ and $J' < 0$) and shows that the ground state is (2, 4, 2) for $J'/J < 2.5$, (3, 4, 1) for $2.5 < J'/J < 5$ and a mixture of spin states (S, S, 0) with $S = 0-4$ for $J'/J > 5$. In the present case, the two interactions are both antiferromagnetic with $J'/J = 1.5$ and the ground state is (2, 4, 2) with the first excited state (3, 4, 1) 7.2 cm^{-1} higher.

Magnetic Interaction. The obtained J values show small Mn(III)−M(II) coupling constants, consistent with the relatively large Mn(III)···M(II) distance. The J' values have also been calculated for **2**−**4** (−8.1, −2.6, and −14.1 cm^{-1}, respectively). The exchange coupling constants for dinuclear copper(II) complexes bridged by a di-μ-hydroxo moiety have been well correlated to the Cu−O−Cu angle and the geometry of the bridging oxygen atom.[25] The small antiferromagnetic coupling observed for **2** is consistent with the Cu−O−Cu angle of 96.9(2)° and the proposed linear relationship to the Cu−O−Cu angle ϕ, where an inversion of the sign of J' is predicted at around $\phi = 97°$.[25]

Scheme 5

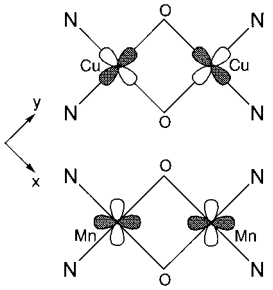

The M(II) ions in **2**, **3**, and **4** have $t_{2g}^6e_g^3$, $t_{2g}^6e_g^2$, and t_{2g}^5 electronic configurations, respectively, and the magnetic orbitals occupy e_g orbitals for **2** and **3** and a t_{2g} orbital for **4**, respectively. Indeed, the interaction between the copper or nickel centers through the oxygen bridging ligand is determined by the overlap of the $d_{x^2-y^2}$ magnetic orbitals of e_g symmetry, and these orbitals are almost orthogonal for the small M(II)−O−M(II) angles around 97−98° observed in **2** and **3** (Scheme 5). On the other hand, the interaction between the low-spin Mn(II) centers is determined by the overlap between the d_{xy} orbitals of t_{2g} symmetry as the unpaired electron of the low-spin Mn(II) ion is expected to occupy the d_{xy} orbital for the axially elongated octahedral coordination around the manganese. The magnetic interaction is symmetrically possible and increases upon decreasing the Mn−O−Mn angle[17a] (Scheme 5). The difference of the nature of the magnetic orbitals involved in this interaction can explain the relatively higher antiferromagnetic coupling found for the low-spin Mn(II)−Mn(II) interaction in **4**. Also note that the antiferromagnetic Mn(II)−Mn(II) (l.s.) coupling, $J' = -14.1$ cm^{-1}, observed in **4** is much higher than the values (2−3 cm^{-1}) found in other hydroxo- and phenoxo-bridged Mn(II)−Mn(II) (h.s.) dinuclear complexes.[20g]

Acknowledgment. This work was supported by Monbusho International Scientific Research Program (Grant No. 10044089 "Joint Research") and by a Grant-in-Aid for Scientific Research on Priority Area (No. 10149101 "Metal-assembled Complexes").

Supporting Information Available: Four X-ray crystallographic files, in CIF format, are available on the Internet only. Access information is given on any current masthead page.

IC980543Y

(25) Crawford, W. H.; Richardson, H. W.; Wasson, J. R.; Hodgson, D. J.; Hatfield, W. E. *Inorg. Chem.* **1976**, *15*, 2107.